Dam seepage analysis based on artificial neural networks: the hysteresis phenomenon.

D. Santillán, J. Fraile-Ardanuy and M.Á Toledo

***Abstract*—Seepage flow measurement is an important behavior indicator when providing information about dam performance. The main objective of this study is to analyze seepage by means of an artificial neural network model. The model is trained and validated with data measured at a case study. The dam behavior towards different water level changes is reproduced by the model and a hysteresis phenomenon detected and studied. Artificial neural network models are shown to be a powerful tool for predicting and understanding seepage phenomenon.**

I. Introduction

THE objective of dam monitoring is to provide data for evaluating dam performance during operation. The typical control variables are deformation, movement, stress, strain, seepage flow rate and turbidity, ground water level, pore water pressure, reservoir and tailwater levels, precipitation, temperature and seismic measurements. Such variables are quantified by means of monitoring instruments installed in the dam.

Given that seepage flow measurements provide useful signs of dam performance, they serve as an important variable in monitoring [1]. The creation of a method for predicting seepage flow rate is a complex task. The medium where it takes place - the dam foundation - is difficult to characterize due to the rock fractures hidden below the surface, the diversity in rock types and the varying degrees of fracture development [2]. Furthermore, the relationship between seepage and its influencing factors is nonlinear. Artificial Neural Networks (ANNs) are useful when complex phenomena require modeling, or when their rules are either partially unknown or very difficult to identify [3].

In this paper a model for predicting seepage flow is developed, based on ANNs trained with recorded data. The seepage behavior is then characterized and analyzed by means of the model, with several conclusions being reached. The influence of the inertia and speed at which the water level changes is studied and a hysteresis phenomenon is detected and discussed.

The main research aim is to analyze the inertia of the response in terms of seepage through dam foundation as the external conditions change over time. This entails the following objectives:

- Testing the ability of the ANNs for modeling seepage through the dam foundation.
- Assessing the usefulness of the ANNs for analyzing the role of different variables involved in dam foundation seepage.
- Evaluating the ANNs as a tool for understanding the real behavior of a system, such as a dam foundation subjected to seepage, in combination with the physical understanding of the system.

II. BACKGROUND

The review of the state of the art is separated in two parts. Firstly, a review of ANNs used in dam applications is presented. Secondly, the seepage flow phenomenon through a fractured rock mass, with the aim of identifying the variables and inertia phenomena involved in the physical problem, is exposed.

A. Artificial Neural Networks

An ANN is a system based on the operation of biological neural networks. It is composed of a large number of simple processing units, termed neurons, which work in a highly interconnected and parallel manner. The result is a nonlinear model which is able to learn, adapt and produce solutions using training data [4].

ANNs have been widely used across science and engineering [5]. Miereles *et al.* in [6] review their industrial applications; Adeli in [7] describes the most common applications in civil engineering; and Waszczyszyn in [8] [9] explains its application to civil and structural engineering problems.

They have also been used in the field of dam engineering. Kim *et al*. in [10] predict the relative crest settlement of concrete-faced rockfill dams with an ANN model. This involves a three-layer perceptron ANN with three input variables, four hidden layers and one output neuron designed for that purpose. Tayfur *et al*. in [11] compare the estimation of water pressure computed with a finite element model and with a multilayered perceptron (MLP) model ANN, concluding that the MLP is as functional as the finite element model. Ahmadi-Nedushan *et al*. in [12] develop a MLP for forecasting displacements of plumblines installed in a concrete gravity dam. Mata in [13] shows a comparison

Manuscript received March 14, 2013. This work was supported by the Ministerio de Medio Ambiente y Medio Rural y Marino (Spanish Environment, Rural and Marine Affairs Ministry) under code 048/RN08/04.5, titled Estudio de la Seguridad de Presas e Identificación de Escenarios de Riesgo mediante Sistemas Inteligentes (SEPRISIS), (Study of Dam Safety and Identification of Risk Scenarios through Intelligent Systems).

D. Santillán is with the Universidad Politécnica de Madrid. Escuela Técnica Superior de Ingenieros de Caminos, Canales y Puertos. Departamento de Ingeniería Civil: Hidráulica y Energética (corresponding author, phone: 34.91.336.67.09; e-mail: david.santillan@upm.es).

J. Fraile-Ardanuy is with the Universidad Politécnica de Madrid. Escuela Técnica Superior de Ingenieros de Telecomunicación. Departamento de Tecnologías Especiales Aplicadas a la Telecomunicación. Avda./ Complutense, 30. 28040 Madrid (e-mail: jfraile@etsit.upm.es)

M Á. Toledo is with the Universidad Politécnica de Madrid. Escuela Técnica Superior de Ingenieros de Caminos, Canales y Puertos. Departamento de Ingeniería Civil: Hidráulica y Energética (e-mail: matoledo@caminos.upm.es)

between multiple linear regression and multilayered perceptron ANN models for the prediction of horizontal displacements recorded by a pendulum in an arch-gravity dam, with the results showing ANN as a good tool in assessment of concrete dam behavior. Miao *et al.* in [14] predict the seepage flow in an earth dam in China, using a multilayered perceptron ANN optimized by a genetic algorithm.

The overall behavior of the ANN depends on the type of neurons and the way they associate with each other in a certain architecture. For seepage flow predictions, an ANN with a functional characteristic of function approximation is suitable. For those proposed, the MLP is chosen given that it is the most used ANN [15] and has been successfully used in the field of dam engineering.

B. Seepage phenomenon analysis.

The three-dimensional seepage field through a fractured rock mass is governed by the hydraulic conductivity of the medium where water flows, by the hydraulic head and by the sources or sinks present in the medium. Seepage also depends on other variables, such as the rock mass stress state [16].

The seepage in a rock mass modifies the stress and stress influences the seepage, as the phenomena are coupled. Two mediums characterize the rock mass: the generalized rock matrix and the connecting fracture network, with different equations that govern the relationships between each field. In the generalized rock matrix, the seepage applies a pressure p_r and a seepage body force f. Each action influences stress in rock mass and can be computed by Eq. (1),

$$\begin{aligned} p_r &= \gamma(H - z) \\ f &= \gamma J_f \end{aligned} \tag{1}$$

in which H is the hydraulic head; z the height relative to the plane of reference; γ , the specific weight of water and J_f the gradient of hydraulic head along the flow.

The stress σ_{ij} changes the volumetric strain ε_V and the porosity n of the rock mass. As a result, the hydraulic conductivity K_r varies and, as a consequence, seepage flow.

$$K_r = K_r(n) \quad ;. \quad n = n(\varepsilon_V) \quad ; \quad \varepsilon_V = \varepsilon_V(\sigma_{ij}) \tag{2}$$

In the connecting fracture network, seepage applies the pressure p_f and the tangent hauling force t_w on the fracture walls to influence stress in rock mass. Eq. (3) govern each action.

$$p_f = n\gamma(H - z) \quad ; \quad t_w = \frac{b}{2} n \gamma J_f \tag{3}$$

Nevertheless, stress changes the apertures of fractures b, which affects the hydraulic conductivity of fractures K_f, which also influences seepage field.

$$K_f = K_f(n) \quad ; \quad b = b(\sigma_{ij}) \tag{4}$$

Seepage and stress are coupled phenomena. A change in the stress field modifies the seepage field and this, in turn, influences the stress field. For this reason, seepage flow prediction models are required such phenomena into account.

III. METHODOLOGY

ANN model design involves selection of the most suitable variables and to determination of its architecture. For calibrating the model, real data are needed. In this research the data was captured from a test case: La Baells Dam. The validation of the model is performed through the use of data not implied in the calibration process. Furthermore, the predictions of the ANN model are compared with those provided by the statistical model that supports the interpretation of the monitoring data at this dam.

A. The case study and statistical model

La Baells Dam is a doubled-arch dam located on the Llobregat River, in the province of Barcelona. It has a maximum height of 102m, a crest length of 403m, and a total reservoir volume of 115hm^3 which supplies water to urban areas. Its thickness varies from 20.1m at the base to 4m at the crest. The drainage basin area is 535km^2, and the design flood peak discharge is 650m^3/s. The dam site is composed of alternating layers of puddingstone and sandstone. The position of the layers is vertical, perpendicular to the riverbed. The puddingstone layers are composed of a mixture of limestone, granite and quartzite, with rounded grains with an average size of 10cm and matrix formed by quadrune.

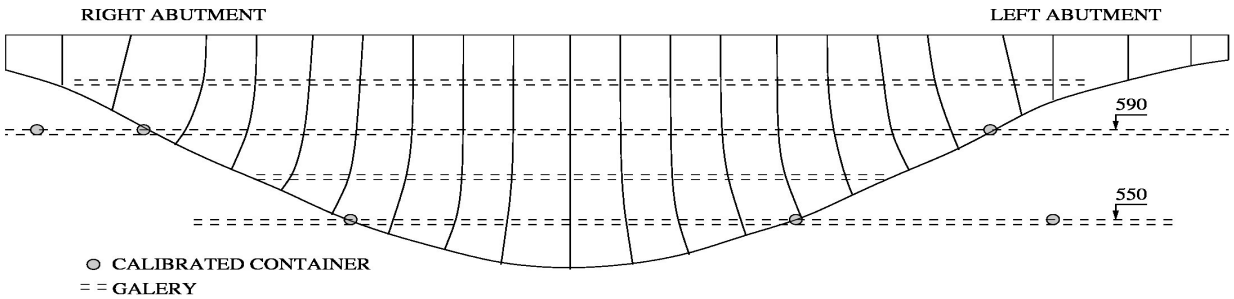

Fig. 1. ketck of La Baells Dam.

Seepage control is fulfilled by 125 drainage boreholes with six reading points composed of calibrated containers. The measurement point chosen for modeling, denominated AFMD550, collects water from the gallery situated in the right abutment at an elevation of 550m (Fig. 1). A statistical seepage flow rate model supports the interpretation of its measurements.

This statistical model establishes a link between a group of variables considered as the cause of the behavior, such as water level in the reservoir and another group of variables that characterizes the structure response of the dam to these actions. The response is quantified by means of instruments installed in the dam which monitor certain parameters such as displacements, strains and seepage flow.

The general expression of the statistical model used at the dam is formulated by Eq. (5), in which V is the response of the dam or variable to predict; β_0, β_i, β_j, and β_k unknown coefficients to determine; t, time in days; T, air temperature; N, water level in reservoir; $f_i(t)$ chronological time functions; $f_j(N)$ water level functions and $f_k(t,T)$ chronological time and air temperature functions.

$$V(t,N,T) = \beta_0 + \sum \beta_i f_i(t) + \sum \beta_j f_j(N) + \sum \beta_k f_k(t,T) \quad (5)$$

Time effects are considered by the functions presented in Eq. (6), where time is measured in days since the beginning of the analysis.

$$\sum \beta_i f_i(t) = \beta_1 t + \beta_2 e^{-t} \quad (6)$$

The effects of water level are usually represented by a polynomial functions, Eq. (7).

$$\sum \beta_j f_j(N) = \beta_3 N + \beta_4 N^2 + \beta_5 N^3 + \beta_6 N^4 \quad (7)$$

The effects of temperature is taken into account by a linear combination of sinusoidal functions which depends on the day of the year, Eq. (8), where d is equal to $2\pi t / 365$. It is assumed that thermal effects can be represented by the sum of sinusoidal functions instead of using temperature measurements [13].

$$\sum \beta_k f_k(t,T) = \beta_7 \sin(d) + \beta_8 \cos(d) + \\ + \beta_9 \sin^2(d) + \beta_{10} \sin(d)\cos(d) \quad (8)$$

Unknown parameters β are estimated by the least-squares method by means of chronological series of recorded data. It should be noted that not all available data are used to fit the model and that the unknown parameters are calculated using a subset of the data termed the fit set. The remaining data, called validation set, assess the model by comparing its output with the real response of the dam in terms of the statistical error test root-mean-square error (RMSE). Table 1 lists the main results of the flow rate statistic model of the

TABLE I
RESULTS OF THE SEEPAGE FLOW STATISTIC MODEL

	Fit set (S1)	Validation set (S2)
Number of data	608	412
RMSE (L/min)	2.9	2.3

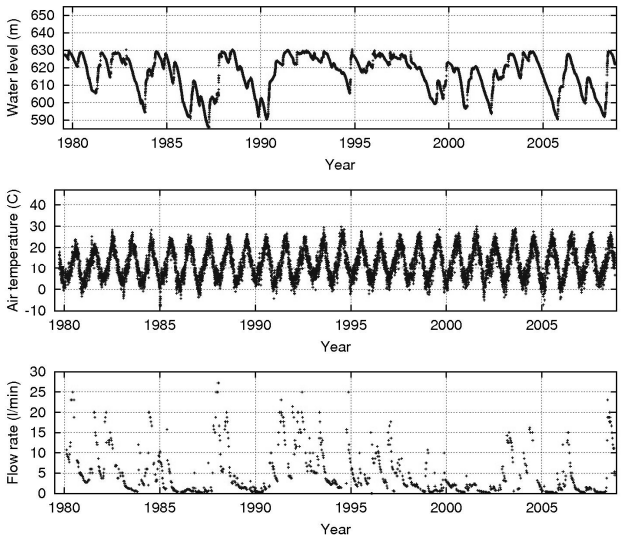

Fig. 2. Available chronological series of data.

selected reading point. RMSE is computed with Eq. (9), in which δ_j^* is the prediction of the j measurement of the variable δ; δ_j, the j measurement of the variable to be predicted and NM, the number of measurements.

$$RMSE = \sqrt{\sum_{j=1}^{N} \frac{(\delta_j - \delta_j^*)}{NM}} \quad (9)$$

Available recorded data are plotted in the Fig. 2. From the top to the bottom they represent the following: water level in the reservoir, air temperature and seepage flow at the selected measurement point. The three variables were measured on 713 different days.

B. Variables that influence seepage phenomenon

Seepage flow is related to the hydraulic head and the hydraulic conductivity of the medium. Temperature, stress and partial derivates of the temperature and hydraulic head with respect to time also influence the seepage flow rate. These partial derivates represent the speed at which rock mass temperature and stress change.

The hydraulic head varies with the water level in the reservoir. The temperature field of the dam is affected by the rock mass temperature and water temperature, and in turn both are influenced by the air temperature. Consequently, the temperature can be characterized in the origin with the variable air temperature. The stress field varies with the hydraulic head and with the temperature. As a result air temperature and water level in the reservoir are considered the most suitable variables to characterize the stress and temperature. The speed at which rock mass temperature and stress change is quantified by simple moving averages of the previous variables, T and N. Initially, the chosen periods are 15, 30, 45, 60, 75 and 90 days for the variable temperature, and seven, 15, 21, 30 and 45 for the water level. The best inputs to the ANN are selected during the training, as explained in the following section.

C. Design of the artificial neural network model

The MLP used in this research has one hidden layer with a tangent sigmoid activation function and one output node whose layer function is linear. Output variable is the seepage flow. However, the best input variables are initially unknown. In a first instance, the input set includes the variables T, the 15, 30, 45, 60, 75 and 90 days simple moving average of T, N and the seven, 15, 21, 30 and 45 days simple moving average of N. The most suitable input variables and the MLP architecture is determined by a backward elimination algorithm whose steps are illustrated in Fig. 3. The relative importance of an input variable is determined by a sensitivity analysis. The algorithm is performed as follows.

In the first step, the available data in the input set are linearly normalized within the range [-1,1]. Subsequently, the data are divided into two sets. The first one, termed training set or D1, is used for training the network and contains 68% of data (425 measurements). The second set, called validation set or D2, is employed for evaluating the prediction of the trained ANN and stores 32% of data (288 measurements). The ratio between the sets is the same as that of the statistical model.

In the second step, the optimal MLP architecture for the given set of input variables is determined. In the first realization of the algorithm all the variables in the input set are considered as inputs. Given the inputs, the MLP architecture is defined by the number of hidden neurons, though there is no general rule for computing that number [3]. A trial-and-error procedure changing the number of hidden units is carried out. The number of hidden nodes is kept to a maximum of twice the number of inputs plus one [17]. The ANNs are trained by means of the Levenberg-Marquardt algorithm and, in order to avoid overfitting and poor generalization, the early stopped method is employed

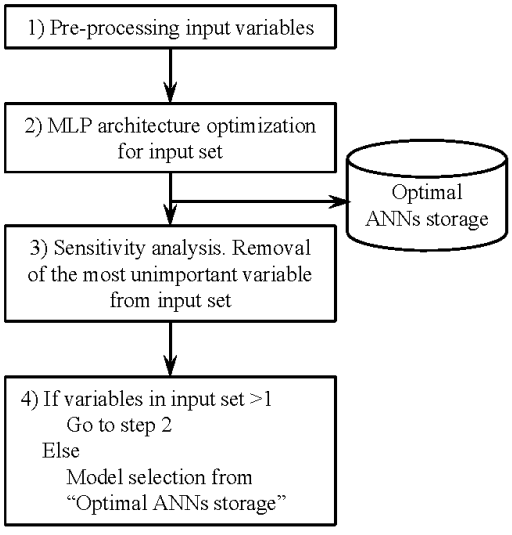

Fig. 3. Flow chart of methodology.

[18]. The network that has the best performance in terms of minimum mean squared error is selected as the optimal for the considered inputs and it is stored.

In the third step, the MLP previously obtained is subjected to a sensitivity analysis in order to eliminate the most unimportant input variable. This is performed by means of the Jacobian matrix defined in Eq. (10), where S_{ik} is the sensitivity of the output y_k due to changes in the input x_i, $f'(net_k)$ and $f'(net_j)$ are, respectively, the derivative of the activation function f(net) taken at the k^{th} output neuron and j^{th} input neuron, w_{ij} is the connection weight between the input neuron i and the hidden neuron j, v_{jk} is the connection weight between the hidden neuron j and the output neuron k and J is the number of hidden neurons. The greater the value of S_{ik}, the more influence there is of the input variable x_i over the output y_k.

$$S_{ik} = \frac{\partial y_k}{\partial x_i} = f'(net_k)\sum_{j=1}^{J} v_{jk} f'(net_j) w_{ij} \tag{10}$$

The influence of the inputs over the output k is measured by the mean square average sensitivities [19], $S_{ik,avg}$, that represent an overall sensitivity of each input variable over the outputs. The input with the lesser value of sensitivity will be assumed to be unnecessary and will be remove from the input set. Should there be input variables, the process returns to step 2 in order to determine the optimal MLP architecture for the new input set, otherwise, to the final step 4.

$$S_{ik,avg} = \sqrt{\frac{\sum_{i=1}^{P} (S_{ik}^{(p)})^2}{P}} \tag{11}$$

Once there is only one input variable and its MLP architecture has been determined, a model among those stored in each iteration is selected in the fourth step. There will be as many models as initial input variables, with different input variables and number of hidden neurons. The network with the best performance in terms of minimum mean squared error is chosen as the final model.

IV. RESULTS

A. Artificial neural network model

The final model selected in the fourth step of the methodology has one hidden layer with four neurons. The input variables are the water level in the reservoir and the seven- and 30-day period moving average of the water level. Table 2 lists the root mean-square errors of the ANN seepage flow rate predictions. The predictions are compared with the measured data in Fig. 4.

TABLE II
RESULTS OF THE SEEPAGE FLOW ANN MODEL

	Fit set (S1)	Validation set (S2)
Number of data	425	288
RMSE (l/min)	2.7	1.3

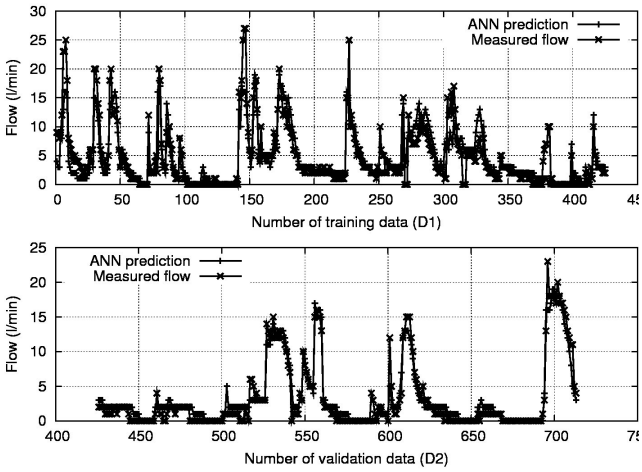

Fig. 4. ANN prediction vs measured data.

B. *Seepage flow*

The prediction of the seepage flow in the measurement point AFMD550 under several situations in the reservoir is computed by the developed ANN model. During a normal operation at La Baells reservoir, the input values of N_a^7 and N_a^{30} (seven and 30-day period simple moving average of the water level on the day *a* respectively) vary within the interval $[N_a\text{-}0.5, N_a\text{+}0.5]$ and $[N_a\text{-}1.0, N_a\text{+}1.0]$ respectively, with N_a being the water level on the day a. Seepage flow is computed within the normal variation intervals of the two simple moving averages for several water levels. The result is plotted in the Fig. 5, which depicts typical values of seepage flow for various values of the water level.

The behavior of the seepage flow is analyzed by means of the model. The evolution of the seepage is computed with the model when the water level rises between two levels, 610 and 624 meters, with three different speeds (Fig. 6). The top chart represents the evolution of the water level over time, whereas the bottom chart the evolution of seepage. Four values of the water level in the reservoir are presented by using points. Each level is plotted three times, with each one corresponding to a different rising speed. The following can be observed:

- For a certain water level in the reservoir, between the values 610 and 624 meters, a higher value of the speed of the water level rise involves a higher value of the seepage flow.

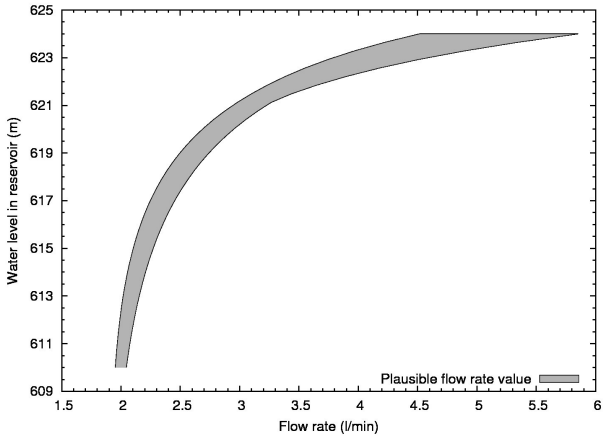

Fig. 5. Seepage flow.

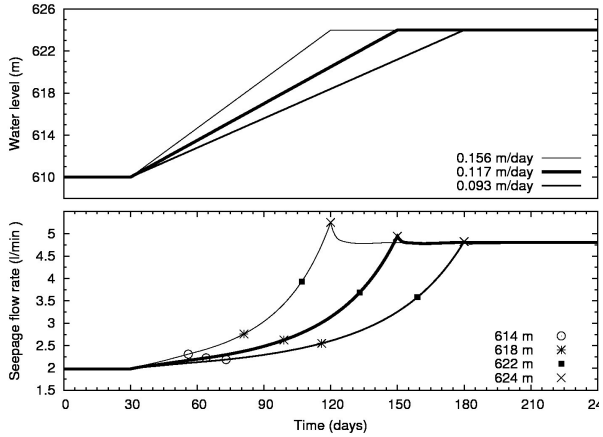

Fig. 6. Seepage flow evolution during a rise of the water level.

- There is a peak of seepage flow at the moment the rise of the water finishes. After that peak, the seepage flow falls to a steady state value that is independent from the rising velocity. If the rising velocity is higher, the flow value of the peak is higher.
- An increment of the water level involves an increment of the seepage flow and vice versa.

In order to check the plausibility of the behavior described by the ANNs, an episode of level change is identified in the recorded monitoring data. A sound example is found between February 2002 and the same month in 2003, with approximate level steps at 614.5, 621.0 and 627.0 (Fig. 7). The peaks predicted by the ANN model are observed in the recorded data with good agreement between both.

Fig. 8 shows the evolution of the seepage, furnished by the model, when the water level falls between 624 and 610 meters, with three different velocities. The following can be observed:

- For a certain water level in the reservoir between the values 624 and 610 meters, as the speed of the level falling was higher, the seepage flow was also higher.
- A decrement of the water level involves a decrement of the seepage flow and vice versa.

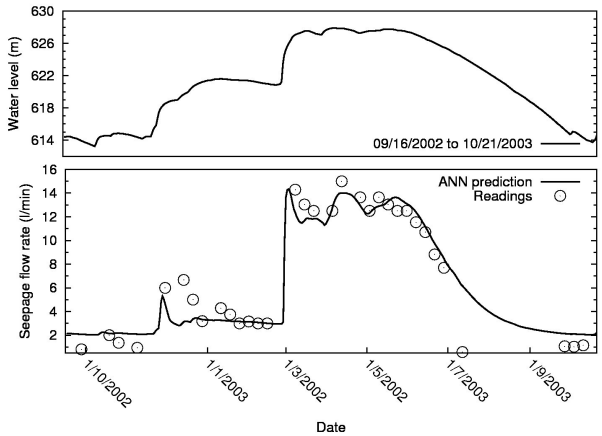

Fig. 7. Measured and computed seepage flow evolution during a period.

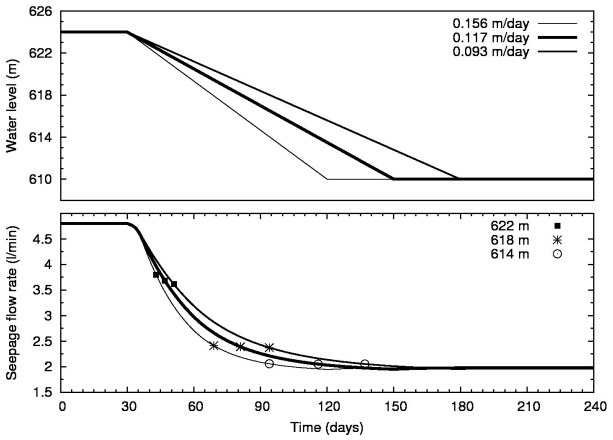

Fig. 8. Measured Seepage flow progress during a fall of the water level computed by ANNs. Water level sinking.

V. DISCUSSION

A. Temperature effect

A double influence of the temperature on seepage should be expected: a) a direct influence on the geometry of the rock fissures due to thermal dilation and contraction and on water viscosity and, b) an indirect influence through the effect on dam stress and deformation that affects the load transmitted to the foundation and hence to the aperture degree of the rock joints. However, no influence of temperature was detected. This has two different but complementary explanations. First, the effect of temperature on seepage could be easily smaller than the accuracy of the measurement instruments. In addition, points located three meters below the ground surface, though above a depth of 10 to 20m (depending upon latitude), undergo annual or seasonal temperature cycles [1]. As the analyzed zone is 42m below the dam crest, it is reasonable to expect no influence of temperature.

B. Inertia effects produced by water level change

The rise of the water level implies an increase of the hydraulic head and gradient. It involves an increment of the measured seepage flow. Moreover, the detected inertia effect and hysteresis influence the seepage flow and are not simple to analyze and explain.

According to the results obtained, the seepage flow measured at any day depends on three significant variables: the water level on the given day and the moving average of seven and 30-day periods. It is remarkable that the moving average of period 15 days was qualified as insignificant, while the seven and 30-day periods were considered significant. This seems to express the inertia effect of two different physical phenomena, one of them more delayed in time corresponding to the 30-day period, and another with a quicker but not immediate response.

In fact, two types of changes are present when water level changes: a) the geometry of the joint system changes as a consequence of the load of the water and the dam on the foundation, and as an effect of the change of the pressure of the water inside the rock joints and b) there is a change in

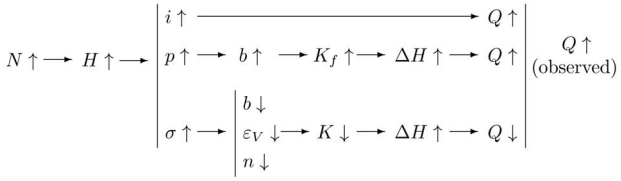

Fig. 9. Sketch of the relation between rising water level and seepage flow.

the flow network. These geometric and hydraulic changes are not independent, though a rather different inertia should be expected for such changes. In addition, from Fig. 6 to Fig. 8 or Table 3 and Table 4, it is clear that the behavior is rather different in the cases of rising and falling water levels. This would suggest that a hysteresis phenomenon is present.

C. Rising water level

An increment of water level in the reservoir implies changes in certain variables, which are sketched in Fig. 9 where the upward-pointing arrows symbolize increases and the downward-pointing arrows decreases. When the water level rises, the hydraulic head increases. Due to the new value of the level, the loads transmitted by the dam to the abutments increase and the stress of the rock mass, the hydraulic gradient and the water pressure also rise. An increment of the hydraulic gradient involves a higher value of the seepage flow.

In addition, an increment of the water pressure forces the joints to open, which increases the hydraulic conductivity of the joints with an accompanying increase in seepage flow. However, a rise of stress σ implies a decrease of the values of certain rock mass features: the volumetric strain, the porosity and the aperture of fractures. These changes reduce the global hydraulic conductivity of the rock mass. Hence, the stress increase involves a decrease in the seepage flow. The effect of the increase of the hydraulic gradient and the stress of the rock mass are opposite. It was observed that a higher water level in the reservoir involves a higher seepage flow. The effect of the hydraulic gradient prevails on the effect of the stress.

A rise of the water level between the values N_0 and N_f will now be analyzed and discussed (Fig. 10). Consideration should be given to the three following hydraulic phases:

TABLE III
SEEPAGE FLOW COMPUYED BY ANNs MODEL. WATER LEVEL RISING

Water level (m)	Velocity of rising (m/day)	Seepage flow (l/min)
614	0.156	2.31
614	0.117	2.22
614	0.093	2.19
618	0.156	2.76
618	0.117	2.62
618	0.093	2.55
622	0.156	3.93
622	0.117	3.68
622	0.093	3.58
624	0.156	5.25
624	0.117	4.95
624	0.093	4.83

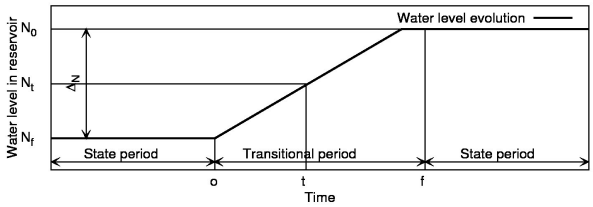

Fig. 10. Increment of water level.

- The initial steady state when the hydraulic head, the stress and the rock mass features do not vary because the water level is constant over time, with a value N_o.
- The transition state when N increase over time.
- The final steady state when the hydraulic head, stress and rock mass features return to a constant value again. It should be noted that this phase starts a long time after the water level has reached the maximum value and maintains constant.

As seen in Fig. 6, for a given value of N, a higher value of the speed of level rising involves a higher seepage flow. Such behavior can be explained in terms of a change in velocity of rock geometry configuration. This would involve consideration of an instant *t* within the transitional state illustrated in Fig. 10 with a water level N_t. If the evolution of the geometry configuration is slower than the evolution of the water level, the aperture of the joints and the volumetric strain at time t are higher than that corresponding to the steady state for the water level N_t. As a result, the seepage flow will be higher too. Due to this phenomenon, a peak in Fig. 6 appears when the water level reaches the final value of 624m.

D. Falling water level

It is clear that a steady lower level implies a lower seepage flow. However, during the transitional state where water level falls from a higher to a lower value, seepage flow also depends on the level decrease velocity. This phenomenon is shown in Fig. 8, where three level decrease velocities are simulated by using the ANN model. It can be observed in the picture that for a given water level, seepage flow grows as the velocity of the level decrease velocity rises. This phenomenon can be checked for three levels: 622, 618 and 614m. In addition, the effect of level decrease velocity is more relevant for the higher level (622m) and becomes less important as the considered level is lower.

It should noted, however, that such a consideration should be treated with care. Given that the reservoir stores water for supplying urban areas, the demand is fairly constant throughout the year, though with a peak in the summer. This involves a narrow variation of the level decrease velocities, which is partly because the stored volume in the reservoir per unit of water level decreases with the latter variable. Hence, for a constant demand, the decrease velocity rises as the level decreases.

VI. CONCLUSIONS

In this paper an artificial neural network type multilayered perceptron is employed for predicting seepage through an arch dam foundation. The network is trained with measured data (over a period of 28 years). Flow rates computed by the multilayered perceptron agree with the observed data. The performance of the model is evaluated in terms of the statistical error test root mean-square error. This is lower than the traditional statistical models that currently support the interpretation of the recorded data. The root mean-square errors of the neural model are 2.7 and 1.3 l/min for the training and validation set, respectively, against 2.9 and 2.3l/min of the statistical model.

TABLE IV
SEEPAGE FLOW COMPUYED BY ANNs MODEL. WATER LEVEL SINKING

Water level (m)	Velocity of rising (m/day)	Seepage flow (l/min)
622	0.156	3.80
622	0.117	3.68
622	0.093	3.61
618	0.156	2.41
618	0.117	2.39
618	0.093	2.37
614	0.156	2.06
614	0.117	2.05
614	0.093	2.05

The artificial neural network model is trained initially with a set of input variables. By means of a sensitivity analysis, the non-influential inputs are detected and removed. As a result, it is detected that temperature has no sensitive effect on seepage in the test case. Such a model also serves as a tool for understanding the behavior of seepage in the test case. It is shown that seepage depends not only on water level in the reservoir, but also on the speed at which it changes. For a certain water level, a higher value of the speed of water level rising involves a higher seepage flow rate.

In conclusion, artificial neural networks are emerging as a powerful tool for predicting and understanding seepage phenomenon. Their easy calibration and use allows them to be a practical tool in dam safety programs. After the study of the behavior of the seepage, several conclusions related to the monitoring process are reached. Changes in seepage can be fast, with maxima and minima. For this reason, continuous data acquisition is necessary, with a reading frequency that enables data capture for each of these situations.

Data should be processed as soon as possible, in order to repeat the collection process if an abnormal value is detected. As a main conclusion, automated monitoring programs seem to be an appropriate choice in the exposed situation. With those systems, data collection and processing frequency can be higher and with low marginal costs.

ACKNOWLEDGMENT

The authors also wish to thank the company *Ofiteco* and l'Agència Catalana de l'Aigua (the Catalan Water Agency) for measured data from La Baells Dam.

REFERENCES

[1] ASCE Task Committee on Guidelines for Instrumentation and Measurements for Monitoring Dam Performance, *Guidelines for instrumentation and measurements for monitoring dam performance*, Reston, VA: ASCE, 2000.

[2] P. Li, W. Lu, Y. Long, Z. Yang and J. Li, "Seepage analysis in a fractured rock mass: The upper reservoir of Pushihe pumped-storage power station in China", *Eng. Geol.*, vol. 97, no. 1, pp. 53-62.

[3] M. Rafiq, G. Bugmann and D. Easterbrook, "Neural network design for engineering applications", *Comput. Struct.*, vol. 79, no. 17, pp. 1541-1552.

[4] B. Martín del Brío and A. Sanz Molina, *Redes neuronales y sistemas borrosos: Introducción teórica y práctica*, Zaragoza, España: Ra-ma, 1997.

[5] I. Flood and N. Kartam, "Neural networks in civil engineering. I: Principles and understanding," *J.Comput.Civ.Eng.*, vol. 8, no. 2, pp. 131-148.

[6] M.R.G. Meireles, P.E.M. Almeida and M.G. Simoes, "A comprehensive review for industrial applicability of artificial neural networks", *IEEE Transactions on Industrial Electronics*, vol. 50, no. 3, pp. 585-601.

[7] H. Adeli, "Neural networks in civil engineering: 1989–2000", *Computer-Aided Civil and Infrastructure Engineering*, vol. 16, no. 2, pp. 126-142.

[8] Z. Waszczyszyn, "Artificial neural networks in civil and structural engineering: Ten years of research in Poland", *Comput. Assis. Mech. Eng. Sci.*, vol. 13, no. 4, pp. 489-512.

[9] Z. Waszczyszyn, "Artificial neural networks in civil engineering: another five years of research in Poland," *Comput. Assis. Mech. Eng. Sci.*, vol. 18, pp. 131-146.

[10] Y. Kim and B. Kim, "Prediction of relative crest settlement of concrete-faced rockfill dams analyzed using an artificial neural network model", *Comput.Geotech.*, vol. 35, no. 3, pp. 313-322.

[11] G. Tayfur, D. Swiatek, A. Wita and V. Singh, "Case Study: Finite Element Method and Artificial Neural Network Models for Flow through Jeziorsko Earthfill Dam in Poland", *J.Hydraul.Eng.*, vol. 131, no. 6, 06/01; 2012/07, pp. 431-440.

[12] B. Ahmadi Nedushan and L. E. Chouinard, "Use of artificial neural networks for real time analysis of dam monitoring data", *Proceedings, Annual Conference - Canadian Society for Civil Engineering*, vol. 2003, pp. 1987-1994.

[13] J. Mata, "Interpretation of concrete dam behaviour with artificial neural network and multiple linear regression models", *Eng. Struct.*, vol. 33, no. 3, 3, pp. 903-910.

[14] X. Y. Miao, J. K. Chu, J. Qiao and L.H. Zhang, "Predicting Seepage of Earth Dams Using Neural Network and Genetic Algorithm", *Advanced Materials Research*, vol. 403, pp. 3081-3085.

[15] S. Haykin, *Neural Networks: A comprehensive foundation*, Upper Saddle River, NJ: Prentice Hall ed. 2, 1998.

[16] C. Junrui, W. Yanqing and L. Shouyi, "Analysis of coupled seepage and stress fields in rock mass around the Xiaowan arch dam", *Communications in Numerical Methods in Engineering*, vol. 20, no. 8, pp. 607-617.

[17] R. Hecht-Nielsen, *Neurocomputing*, New York, NY: Addison-Wesley Publishing Company,1990.

[18] H. Demuth, M. Beale and M. Hagan, *Neural Network Toolbox 6. User's Guide*, Natick, MA: The MathWorks.

[19] J.M. Zurada, A. Malinowski and S. Usui, "Perturbation method for deleting redundant inputs of perceptron networks", *Neurocomputing*, vol. 14, no. 2, pp. 177-193.